Comparison of MRI and MIBI SPECT as Modalities for Infarct Size Assessment

Je'nine Horn   ND Rad (D); ND Rad (NM); B Tech NM (cum laude)

Abstract

BACKGROUND: According to the National Heart, Lung and Blood Institute, coronary artery disease (CAD) is the leading cause of death in the Western world [1]. This study compares 99m-technetium-methoxyisobutylisonitrile single photon emission computed tomography ([99m]TC-MIBI SPECT) and magnetic resonance imaging (MRI) as myocardial infarct size imaging modalities as a means to assess extent of CAD. The study is underpinned by recent publications which are discussed in this article [1-7].

METHOD: Five patients, four males and one female, aged 40-65 years who were hospitalized for myocardial infarction were participants in this study. Patients underwent a ^{99m}Tc-MIBI SPECT stress study to detect if a myocardial defect was present. Patients with defects on ^{99m}Tc-MIBI SPECT stress studies then underwent ^{99m}Tc-MIBI SPECT rest studies, to distinguish between ischemia and infarction. The patients with defects on ^{99m}Tc-MIBI SPECT rest studies then underwent further contrast-enhanced MRI studies. The MRI and ^{99m}Tc-MIBI SPECT rest infarction sizes were drawn as regions of interest (ROI). The infarct size was expressed as a percentage relating the infarcted area to the entire area of the left ventricle for both the MRI and the rest ^{99m}Tc-MIBI SPECT studies.

RESULTS: The average global ^{99m}Tc-MIBI SPECT infarction size in percentage in the 5 patients was 21% and the MRI global average infarction size was 18%.

CONCLUSION. The MRI and rest ^{99m}Tc-MIBI SPECT global infarction size percentages have shown a good correlation.

Keywords: Coronary artery disease, ^{99m}Tc-MIBI SPECT, magnetic resonance imaging, infarction.

Introduction

According to the National Heart, Lung and Blood Institute coronary artery disease (CAD) is the leading cause of death in the Western world [1]. Patients who are not diagnosed with CAD, a potentially reversible cause of heart disease, may be at risk of developing progressive cellular damage, heart failure and death [5]. The therapy and prognosis of CAD are increasingly being guided by the accurate and early detection of viable myocardium [4]. There are risks associated with revascularization. Patients with heart failure are unlikely to benefit from revascularization, this can be avoided by discrimination between viable and nonviable dysfunction [4]. Hence the search for a reliable ultimate noninvasive test to detect CAD [1]. This test should have the potential to reduce the number of unnecessary invasive angiographic procedures leading to a better patient outcome and consequently decreasing the cost of care for cardiovascular disease [1].

Technetium-99m-labeled imaging agents are being increasingly used because of their improved imaging properties in the evaluation of tissue viability with single photon emission computed tomography (SPECT). The energy window, reduced scatter, less attenuation artifacts and improved spatial resolution of ^{99m}Tc make it highly useful [5]. A variety of other imaging techniques, such as magnetic resonance imaging (MRI) have recently been introduced for the clinical use as promising viability tests [6]. One of these techniques, which is a well-established method for evaluating cardiac morphology and function, is MRI [7].

Contrast MRI is used to assess delayed hyper-enhancement as a marker of scar tissue and to assess contractile reserve [6]. Areas of reduced contrast enhancement can be seen as hypo-enhanced in the endocardial core of the infarct which indicates microvascular obstruction. This can be seen after first-pass images that are performed immediately after contrast injection [3]. Regional area signal hyper-enhancement indicating myocardial necrosis can be seen on delayed images, namely 10 to 20 minutes after contrast injection [3]. Delayed hyper-enhancement is correlated with poor recovery of contractile function after revascularisation in patients with chronic myocardial infarction [3]. Therefore, hyper-enhancement can be used as a constant marker for nonviable myocardium [3]. The ideal diagnostic test for assessing myocardial viability must adhere to the following requirements namely:

- accurate,
- easily accessible,
- cost-effective, and
- convenient for patients [6].

For this reason the ideal noninvasive diagnostic myocardial viability test has yet to be found [6].

MRI and MIBI are compared in this study to assess their appropriateness as myocardial viability test modalities.

Method

- **Patient population:** The study included five patients (four males and one female, aged 40-65 years) hospitalised for MI. These patients were diagnosed by acute chest pain, increased creatine phosphokinase levels and characteristic electro-cardiograph (ECG) changes. To be included in the study, patients had to have no contra-indications for undergoing an MRI examination. All patients gave written, as well as verbal informed consent for the study .

- **Study protocol:** All the patients (n=5) had undergone a ^{99m}Tc-MIBI SPECT stress study to detect if a myocardial defect was present. Patients with defects on ^{99m}Tc-MIBI SPECT stress studies further underwent ^{99m}Tc-MIBI SPECT rest studies to differentiate between ischemia and infarction. The patients with defects on ^{99m}Tc-MIBI SPECT rest studies were then referred for contrast-enhanced MRI.

- **[99m]Tc-MIBI Gated SPECT protocol:** All the patients underwent both stress and rest ^{99m}Tc-MIBI Gated SPECT studies to differentiate between myocardial ischemia and infarction. Imaging started thirty minutes after intravenous injection (IV) of 925 Mega-Bequerell (MBq) ^{99m}Tc-MIBI. To improve the overall quality of the heart images fifty grams of white chocolate were given to clear the gallbladder of all the radio-activity. The stress gated SPECT studies were performed 60 minutes post intravenous injection of ^{99m}Tc-MIBI. The rest gated SPECT studies were performed post 24 hours after stress studies. A dual head Siemens Multispect II, equipped with low-energy, high resolution parallel-hole (LEHR) collimators was used. The energy discrimination was centered on 140 kilo-electron Volt (keV) with a 30% window. A total of 64 projections over 360 degrees were obtained in a 64 x 64 matrix with 40 seconds (s) per view. At each projection, 8 electro-cardiographic gated frames per cardiac cycle were acquired. For image

reconstruction after projection data was pre-filtered using a Butterworth filter (order, 8; cut-off frequency, 0.4 cycles per centimeter). Filtered back-projection was also performed using a ramp filter.

- **MRI protocol:** MRI was performed with a General Electric, Signa CV equipped with a 1.5-Telsa (T) magnet by using a phased-array coil wrapped around the chest was used. After localization of the heart, 9 contiguous tagged short-axis cine images of the left ventricle (LV) were prescribed to cover the entire heart from the base to the apex. Tagged images were acquired by using an electro-cardiac-graph (ECG) gated segmented k-space gradient echo pulse sequence with spatial modulation of magnetization. Image parameters were as follows: repetition time (TR) 5.8 milli-seconds (ms), excitation time (TE) 2.3 ms, image matrix 256 x 128, field of view 35cm (centimeter), slice thickness 9 millimeter (mm), spacing 2 to 4mm, flip angle 12°, and k-space/cardiac cycle 8 to 12 lines. Images were acquired during short breath-holding (12 to 15 seconds) at expiration. After tagged images were acquired, the patients received an intravenous bolus 20 milli-moles per kilogram (mmol/kg) of magnevist. The first-pass perfusion is seen as the 0-minute image. Short-axis images were also acquired on 5-, 10- and 15 minutes post-contrast injection.

Data analysis

The MRI images were transferred from DICOM to the Icon workstation (see Figure 1). The MRI images were analyzed in display mode and the 99mTc-MIBI rest images were analysed in the cardiac pictogram mode. The MRI infarction size was drawn as a region of interest (ROI) on the all of the 15 minutes after contrast administration images.

Figure 1. One of the MRI images of the left ventricle displayed on the Icon workstation (Courtesy of Universitas Hospital).

The MRI infraction area on the 15-minute contrast administration can be seen as a hyper-enhanced area on the images. The MRI image color was changed from black and white to hot metal on the display table as it made it easier to distinguish the hyper-enhanced infarction area (see Figure 2).
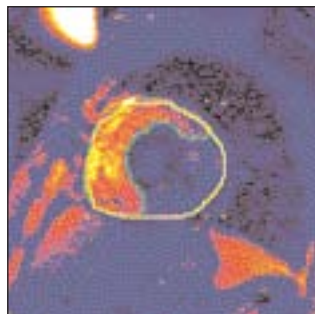

Figure 2. The MRI image of the left ventricle and the infarction size drawn with the image colouron hot metal (Courtesy of Universitas Hospital).

The hyper-enhanced infarction area showed red on the hot metal with MRI. The 99mTc-MIBI rest images were also viewed on the hot metal color. The infarction area which received no perfusion, in
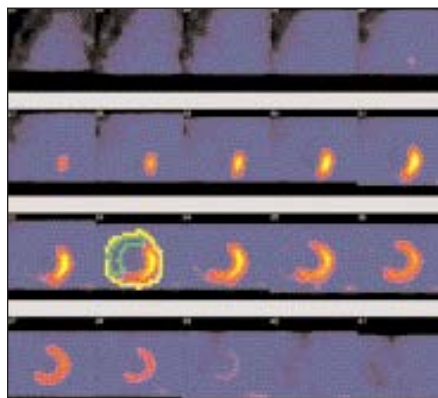

Figure 3. The 99mTc-MIBI SPECT rest cardiac pictogram images with the infarction size and the left ventricle drawn as the regions of interest (Courtesy of Universitas Hospital).

contrast with the MRI, is seen as a black area (see Figure 3). The infarct size was expressed as a percentage of the infarction area over the entire area of the left ventricle for both the MRI and the rest 99mTc-MIBI SPECT, i.e.

Sinfarction (%) = Pixelsinfarction/Pixelsleft ventricle x 100% [1].

The left ventricle and the infarction size was measured on all the MRI and rest 99mTc-MIBI SPECT images. All the MRI and rest 99mTc-MIBI SPECT images were calculated to obtain a global infarction size in percentage.

Statistical analysis

The Standard Deviation (SD) was used for all the MRI and 99mTc-MIBI Gated SPECT values. Single factor Analysis of Variance (ANOVA) was used to compare the global rest 99mTc-MIBI SPECT and MRI infarction size percentages.

Results

The infarction size percentages of patients 4 and 5 on the 99mTc-MIBI Gated SPECT was higher than that of the MRI. MRI infarction size percentages of patients 1, 2 and 3 were higher on the MRI, than in the case of 99mTc-MIBI Gated SPECT (see Table I). The average global MIBI infarction size percentages in the 5 patients was 21 and the MRI global average infarction size was 18%. The MRI and
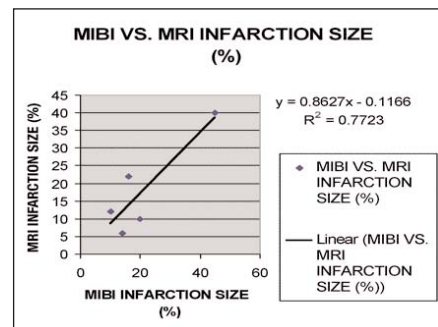

Figure 4. The 99mTc-MIBI SPECT rest infarction size percentages versus the MRI infarction size percentages (Courtesy of Universitas Hospital).

99mTc-MIBI infarction size percentages use significant digits showed good correlation (see Figure 4).

Discussion

Both 99mTc-MIBI Gated SPECT and the MRI demonstrate advantageous characteristics to show myocardial tissue viability. MRI has the advantage of demonstrating higher quality anatomical images, but is a very expensive imaging modality. The 99mTc-MIBI Gated SPECT, although producing lower quality anatomical images than that of the

PATIENT	99mTc-MIBI GATED SPECT INFARCTION SIZE %	MRI INFARCTION SIZE %
1	10	12
2	6	14
3	16	22
4	20	10
5	45	40
Table I. The infarction size percentages of 99mTc-MIBI Gated SPECT and MRI.		

MRI, is easily accessible, cost-effective and convenient for patients. There were some limitations to the study. The study population was small due to the high cost of MRI examinations and the three examinations the patients had to undergo, namely the stress 99mTc-MIBI, the rest 99mTc-MIBI to indicate if myocardial infarction was present, and a myocardial MRI. The discrepancy between MRI and SPECT could possibly be as a result of the region of interest (ROI) drawn being dependent on the operator's skill and knowledge of MRI and 99mTc-MIBI imaging modalities.

Conclusion

As CAD remains one of the leading causes of death in the Western world indicating the need for good quality, reliable noninvasive myocardial imaging modality. Since scar tissue (infarction) in the myocardium is unlikely to benefit from revascularization, it is important to determine the extent and size thereof. Due to the characteristics of the MRI and rest 99mTc-MIBI SPECT it was decided to compare their global infarction size percentages in the search for the ultimate myocardial imaging modality. The MRI and rest 99mTc-MIBI SPECT global infarction size percentages showed a good correlation with only a 2% differentiation between their global infarction size percentages. Therefore, both the MRI and the MIBI scintigraphic imaging modalities infarction size percentages correlate in such a way that it may be used for myocardial viability diagnosis.

References

1. Bogaert, J. (ed.), Duerinckx, A.J. (ed.) & Rademakers, F.E. (ed.). 2000. *Magnetic Resonance of the Heart and Great Vessels.* Berlin, Germany: Springer. 123-137.

2. Eisner, R.L. & Patterson, R.E. 1999. The challenge of quantifying defect size and severity: Reality versus algorithm. *Journal Nuclear Cardiology*, 6(3): 362-371.

3. Gerber, B.L., Garot, J., Bluemke, D.A., Wu, K.C. & Lima, J.A.C. 2002. *Accuracy of Contrast-Enhanced Magnetic Resonance Imaging in Predicting Improvement of Regional Myocardial Function in Patients After Acute Myocardial Infarction.* Accessed 27 November 2002. http://circ.ahajournals.org/cgi/content/full/106/9/103

4. Shan, K., Constantine, G., Sivananthan, M.D. & Flamm, S.D. 2004. Role of Cardiac Magnetic Resonance Imaging in Assessment of Myocardial Viability. *Circulation*, 109: 1328-1334.

5. Marcelo(F.D.C. 2003. The quest for myocardial viability: Is there a role for nitrate-enhanced imaging? *Journal Nuclear Cardiology*, 10(6): 696-699.

6. Matsunari, M.D., Taki, J. & Tonami, N. 2002. Sequential Strategy Using Multimodality viability Test: Does It Work? Accessed 23 July 2004. http://jnm.snmjournals.org/cgi/conent/full/43/6/803

Oshinski, J.N., Han, H.C., Ku, D.N. & Pettigrew, R.I. 2001. Quantitative Prediction of Improvement in Cardiac Function after Revascularization with MR Imaging and Modeling: Initial Results. Accessed 23 July 2004. http://radiology.rsnajnls.org/cgi/content/full/221/2/515

CPD past answers

Answers April 2005 issue	Answers November 2005 issue
Question 1 - (c)	Question 1 - (c)
Question 2 - (a)	Question 2 - (c)
Question 3 - (a)	Question 3 - (c)
Question 4 - (b)	Question 4 - (b)
Question 5 - (b)	Question 5 - (d)
Question 6 - (c)	Question 6 - (b)
Question 7 - (a)	Question 7 - (c)
Question 8 - (a)	Question 8 - (c)
Question 9 - (c)	Question 9 - (c)
Question 10 - (c)	Question 10 - (b)
Question 11 - (c)	Question 11 - (a)
Question 12 - (a)	Question 12 - (b)
Question 13 - (b)	Question 13 - (b)
Question 14 - (a)	Question 14 - (a)
Question 15 - (a)	Question 15 - (b)
Question 16 - (b)	Question 16 - (a)
Question 17 - (b)	Question 17 - (d)
Question 18 - (c)	Question 18 - (a)
Question 19 - (c)	Question 19 - (b)
Question 20 - (a)	Question 20 - (c)